Electronic structures and energy band properties of Be- and S-doped wurtzite ZnO*

Zheng Shu-Wen(郑树文)†, Fan Guang-Han(范广涵), He Miao(何 苗), and Zhang Tao(张 涛)

Laboratory of Nanophotonic Functional Materials and Devices, Institute of Opto-electronic Materials and Technology, South China Normal University, Guangzhou 510631, *China*

(Received 11 November 2013; revised manuscript received 22 February 2014; published online 20 April 2014)

The energy band properties, density of states, and band alignment of the $Be_xZn_{1-x}O_{1-y}S_y$ alloy (Be- and S-doped wurtzite ZnO) are investigated by the first-principles method. $Be_xZn_{1-x}O_{1-y}S_y$ alloy is a direct band gap semiconductor, the valence band maximum (VBM) and the conduction band minimum (CBM) of $Be_xZn_{1-x}O_{1-y}S_y$ are dominated by S 3p and Zn 4s states, respectively. The band gap and lattice constant of $Be_xZn_{1-x}O_{1-y}S_y$ alloy can be modulated by changing the doped content values x and y. With the increase in Be content value x in the $Be_xZn_{1-x}O_{1-y}S_y$ alloy, the band gap increases and the lattice constant reduces, but the situation is just the opposite when increasing the S content value y in the $Be_xZn_{1-x}O_{1-y}S_y$ alloy. Because the lattice constant of $Be_{0.375}Zn_{0.625}O_{0.75}S_{0.25}$ alloy is well matched with that of ZnO and its energy gap is large compared with that of ZnO, so the $Be_{0.375}Zn_{0.625}O_{0.75}S_{0.25}$ alloy is suitable for serving as the blocking material for a high-quality ZnO-based device.

Keywords: first-principle, $Be_xZn_{1-x}O_{1-y}S_y$ alloy, electronic structure, band gap modulation

PACS: 63.20.dk, 73.20.At, 71.15.Mb, 71.20.Be **DOI:** 10.1088/1674-1056/23/6/066301

1. Introduction

Zinc oxide (ZnO) is an important wide-band-gap semiconductor ($E_g = 3.37$ eV) and has a large exciton binding energy (~ 60 meV) that can be used to fabricate high power and high-frequency optoelectronic devices, such as light-emitting diodes, laser diodes, and solar cells.[1–3] A high-efficiency ZnO device needs a stable p-type material and good device structure, such as quantum wells and superlattices. Fortunately, the reliable and stable p-type ZnO material can be grown using arsenic as the dopant.[4] So, the next step is to obtain a good device structure, which is correlated with the band gap engineering. Doping is an effective way of engineering the band gap.

The band gap can be modified by the substitution of isoelectronic cations or anions in ZnO. Most experimental and theoretical researches focus on cations-substituted alloys, for example, MgZnO, ZnCdO, and BeZnO alloys are doped to substitute the Zn sites. Due to the difference in crystal structure between MgO (cubic) and ZnO (hexagonal), the solubility of Mg in ZnO is rather limited (0.36 in atomic concentration).[5,6] A similar situation also appears in the ZnCdO alloy and the upper limit of Cd concentration is 0.25.[7] However, doping Mg into ZnO can increase the band gap while doping Cd can reduce the band gap. In fact, BeZnO alloy has advantages over MgZnO and ZnCdO alloys because ZnO and BeO have the same hexagonal wurtzite structures, so BeZnO alloy may be a good candidate for band gap modulation from 3.37 eV to 10.6 eV, which has been confirmed experimentally.[8] But the lattice mismatch between ZnO and BeO is quite large (about 19% for a and c) because their ionic radii are quite different (Be^{2+} is 0.27 Å while Zn^{2+} is 0.60 Å), which will lead to a large formation energy and induce a tendency of disordered phase.[9] In order to suppress the disordered phase of BeZnO alloy, some research work has been done. Doping Mg into the BeZnO alloy is investigated and regarded as a good method, proved theoretically[10,11] and experimentally,[12] which is because the Mg–O bond length is longer than Zn–O's. Doping Ca into the BeZnO alloy to replace the Zn site is also a solution because the ionic radius of Ca^{2+} is larger than that of Zn^{2+}.[13]

Other work focused on band gap engineering of ZnO that is doped by S, Se or Te atom to replace the O atom to form ZnOS, ZnOSe or ZnOTe alloys respectively,[14] but more researchers have studied ZnOS alloy because the ionic radius difference is smaller between S^{2-} (1.84 Å) and O^{2-} (1.40 Å), and they are easier to replace than doping Se^{2-} (1.98 Å) and Te^{2-} (2.21 Å).[15] It is also possible to suppress the disordered phase of BeZnO alloy by doping S into the BeZnO alloy. When S doping concentration is 0∼0.45, the band gap of the ZnOS alloy can be adjusted from 3.37 eV to 2.6 eV.[16,17] Doping not only adjusts the band gap but also changes the lattice parameter. When doping S into ZnO, the lattice constants become larger,[17] but the lattice constants become smaller when

*Project supported by the National Natural Science Foundation of China (Grant No. 61078046), the Special Funds for Provincial Strategic and Emerging Industries Projects of Guangdong Province, China (Grant No. 2012A080304016), and the Youth Foundation of South China Normal University, China (Grant No. 2012KJ018).

†Corresponding author. E-mail: LED@scnu.edu.cn

© 2014 Chinese Physical Society and IOP Publishing Ltd

doping Be into the ZnO.[8] So the lattice constants of Be and S co-doped ZnO may be matched with those of ZnO, which is important for fabricating a high-quality ZnO-based structure. To the best of our knowledge, so far a study about Be and S co-doped ZnO has not yet been reported in the literature.

In this work, the energy band properties and density of states (DOS) of the $Be_xZn_{1-x}O_{1-y}S_y$ alloy are investigated in detail. In Section 2, a brief description of the computational method is given. The energy band properties and density of states (DOS) are discussed in Section 3. The formation energy and the band alignment of the $Be_xZn_{1-x}O_{1-y}S_y$ alloy are also analyzed in Section 3. Finally, the summary of our main results are given in Section 4.

2. Computational methods

The calculations are based on density functional theory (DFT) with the plane-wave pseudo-potential method as implemented in the CASTEP (Cambridge Serial Total Energy Package) code.[18] The exchange–correlation function adopts the Perdew, Burke, and Ernzerhof (PBE) functional in the generalized gradient approximation (GGA).[19] The interaction between valence electron and ion core is described by an ultrasoft pseudo-potential. The valence atomic configurations are $3d^{10}4s^2$ for Zn, $2s^22p^4$ for O, $2s^2$ for Be, and $3s^23p^4$ for S, respectively. An energy cutoff for the plane wave expansion is set to be 400 eV and a 4×4×5 k point Monkhorst–Pack[20] mesh is performed for the Brillouin zone integration in reciprocal space. The ideal ZnO has a hexagonal wurtzite structure with the space group C_{6v}^4–$P6_3mc$. In order to simulate the wurtzite $Be_xZn_{1-x}O_{1-y}S_y$ alloys, our computational models are shown in Fig. 1. The 16-atom supercell (2×2×1) of the wurtzite ZnO is used for $Be_{0.125}Zn_{0.875}O$ by replacing the Zn site with a Be atom, $ZnO_{0.875}S_{0.125}$ by replacing the O site with an S atom, and $Be_{0.125}Zn_{0.875}O_{0.875}S_{0.125}$ by replacing the Zn site and the O site with a Be atom and an S atom, respectively. A 32-atom supercell (2×2×2) of the wurtzite ZnO is used for $Be_{0.375}Zn_{0.625}O_{0.75}S_{0.25}$ by replacing Zn sites and O sites with three Be atoms and two S atoms, respectively. Before calculating the band structure and DOS of the $Be_xZn_{1-x}O_{1-y}S_y$ alloy, the crystal structures of the models are optimized by the BFGS[21] minimization algorithm and the optimization will finish when the convergence criterion is satisfied. (The total energy is less than 1×10^{-5} eV/atom, the atom internal stress is below 0.05 GPa, the force on each atom and the displacement of each atom are below 0.03 eV/nm and 0.001 nm, respectively.)

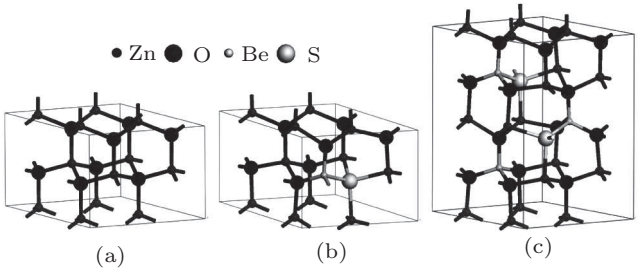


Fig. 1. Structural models for wurtzite $Be_xZn_{1-x}O_{1-y}S_y$ alloy, showing ZnO (2×2×1) supercell (a), $Be_{0.125}Zn_{0.875}O_{0.875}S_{0.125}$ model (b), and $Be_{0.375}Zn_{0.625}O_{0.75}S_{0.2}$ model (c).

3. Results and discussion

3.1. Structural properties

For the considered structures, we perform the structural optimization by minimizing the total energy with respect to the supercell parameters. The structural parameters (a, c, and supercell volume V) and the values of supercell total energy E_{tot} for ZnO, $Be_{0.125}Zn_{0.875}O$, and $ZnO_{0.875}S_{0.125}$ are listed in Table 1. As can be seen, the lattice constants $a = 3.282$ Å and $c = 5.296$ Å for the wurtzite ZnO are in good agreement with the experimental data[22] and other calculated values,[23,24] which indicates that the calculated method is reasonable. It is found that the structural parameters a, c, and V of the $Be_{0.125}Zn_{0.875}O$ alloy are smaller than those of ZnO, which is consistent with the scenario in Ref. [24], but it is contrary to the scenario for $ZnO_{0.875}S_{0.125}$ alloy, which has been proved experimentally.[25] The reversed change is mainly due to the ionic radius differences between Zn and Be ions or between O and S ions. At the same time, the supercell total energies of $Be_{0.125}Zn_{0.875}O$ and $ZnO_{0.875}S_{0.125}$ alloys are higher than that of ZnO, which reveals that the structural stabilities of the BeZnO and ZnOS ternary alloys are declined after Be or S has been doped into ZnO.

Table 1. Calculated structural parameters and total energies of wurtzite ZnO, $Be_{0.125}Zn_{0.875}O$, and $ZnO_{0.875}S_{0.125}$ alloys.

Name		Lattice constant		Supercell volume V/Å^3	Supercell total energy E_{tot}/eV
		a/Å	c/Å		
ZnO	This work	3.282	5.296	197.631	–17178.614
	Exp.[22]	3.249	5.206		
	Calc.[23]	3.283	5.309		
	Calc.[24]	3.280	5.297		
$Be_{0.125}Zn_{0.875}O$		3.214	5.185	185.573	–15501.519
$ZnO_{0.875}S_{0.125}$		3.350	5.417	210.570	–17020.053

3.2. Band structure and DOS

The band structure can provide useful information to explain some physical properties of a material, so its experimental measurement or theoretical calculation is essential. For comparison, the band structure and density of states (DOS) of wurtzite ZnO are first studied. The calculated band structure is shown in Fig. 2(a). It is evident that the bottom of the conduction band and the top of the valence band are located at the Γ symmetry point, which indicates that ZnO is a semiconductor with a direct band gap. The calculated band gap is about 0.744 eV, which is smaller than the experimental value (3.37 eV[22]). In fact, the underestimation of the band gap is a well-known drawback of the standard DFT calculation, but the band gap can be corrected by the scissors approximation,[26] and the calculated value is also advisable for the qualitative analysis. Our calculated band gap value is consistent with those in previous studies.[23,24]

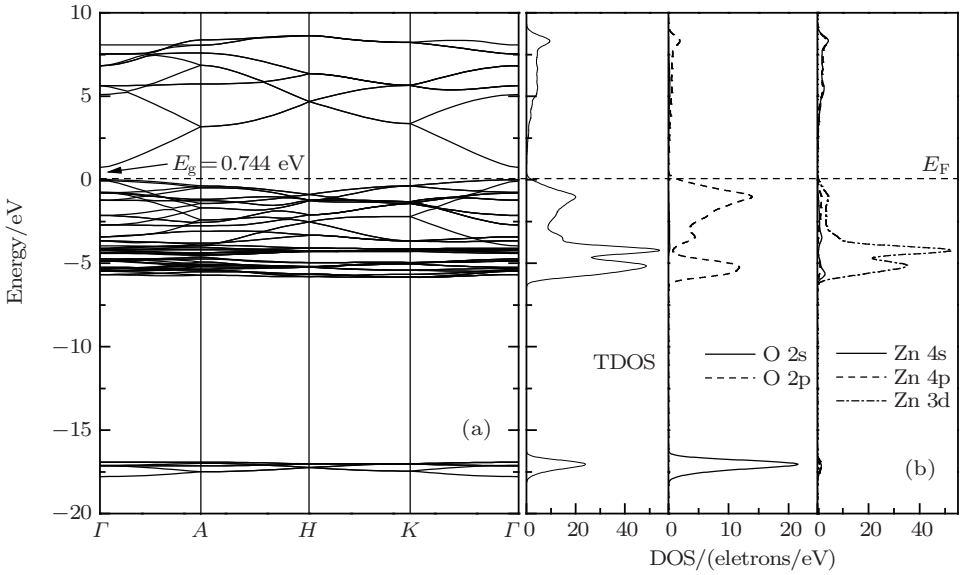


Fig. 2. Calculated band structure (a) and total DOS and partial DOS (b) of wurtzite ZnO. The k symmetry points are $\Gamma(0,0,0)$, $A(0,0.5,0)$, $H(0,0.5,0.5)$, and $K(0,0,0.5)$. Fermi level is set to be zero.

The DOS gives an insight into the band structure. Figure 2(b) displays the total DOS and partial DOS of Zn and O atoms for ZnO in the range from −20 eV to 10 eV. It is clear that the valence band can be divided into two parts: the upper valence band (from −6.6 eV to 0 eV) and the lower valence band (from −18.5 eV to 16 eV). The lower valence band comes from the O 2s state and is far from the top of the valence band, so its influence on the energy gap can be ignored. The upper valence band is mainly occupied by O 2p and Zn 3d states, but dominating the valence band maximum (VBM) is the O 2p state. The conduction band is chiefly contributed by Zn 4s4p and O 2p states, and the Zn 4s state dominates the conduction band minimum (CBM). So the band gap of pure ZnO is determined by O 2p and Zn 4s states. In fact, the strong p–d repulsion between O 2p and Zn 3d states in the upper valence band causes the VBM to approach the conduction band, reducing the band gap. The calculated DOS distribution of pure ZnO is in agreement with the previous research result.[10]

Figures 3 and 4 are the calculated band structures and DOS of $Be_{0.125}Zn_{0.875}O$ and $ZnO_{0.875}S_{0.125}$ alloys, respectively. It is found that the two alloys are both direct semiconductors because the CBM and VBM are at the same k-point (Γ). The band gap (1.102 eV) of $Be_{0.125}Zn_{0.875}O$ is larger than that of ZnO, which is comparable to those reported by Fan *et al.*[28] We can explain it according to the total DOS and partial DOS distributions (in Fig. 3(b)). The upper valence band mainly consists of O 2p, Zn 3d, and Be 2s2p states, but the O 2p state dominates the VBM. The conduction band is occupied by the O 2p state, Zn 4s4p state, and a small number of Be 2s2p states, but the CBM is dominated by the Zn 3s state, which is similar to the scenario of pure ZnO. The p–d repulsion mechanism in the upper valence band of $Be_{0.125}Zn_{0.875}O$ becomes weakened, compared with that in pure ZnO, because Zn 3d electron numbers are reduced from 79.62 electrons of ZnO to 69.7 electrons of $Be_{0.125}Zn_{0.875}O$, which makes the VBM shift toward a lower energy, being helpful to increase the band gap. For the $ZnO_{0.875}S_{0.125}$ alloy as shown in Fig. 4, the calculated band gap is about 0.701 eV, which is slightly smaller than that of pure ZnO. It is found that the valence band of $ZnO_{0.875}S_{0.125}$ can be divided into three parts: the upper valence band, the middle valence band, and the lower valence band, which is different from those of ZnO and $Be_{0.125}Zn_{0.875}O$. The lower valence band is dominated by

the O 2s state and the middle valence band is occupied by the S 3s state. Their electron distributions show strong local features and are far from the top of the valence band, so their effects on the band gap are negligible. The upper valence band of $ZnO_{0.875}S_{0.125}$ is composed mostly of O 2p, S 3p, and Zn 3d states, and the p state number (39.378 electrons from O 2p and S 3p states) of the upper valence band is more than the p state number (36.69 electrons from the O 2p state) of ZnO. Hence the p–d repulsion of $ZnO_{0.875}S_{0.125}$ is enhanced more than that of ZnO, thereby pushing up the VBM toward a higher energy level and making the band gap narrower. Owing to the S 3p state occupying the higher energy than the O 2p state, the properties of the VBM of $ZnO_{0.875}S_{0.125}$ are determined by the S 3p state. The conduction band of $ZnO_{0.875}S_{0.125}$ is composed chiefly of Zn 4s4p, O 2p, and S 3p states, but the bottom of the conduction band is occupied by Zn 4s, which is the same as the scenarios of ZnO and $Be_{0.125}Zn_{0.875}O$.

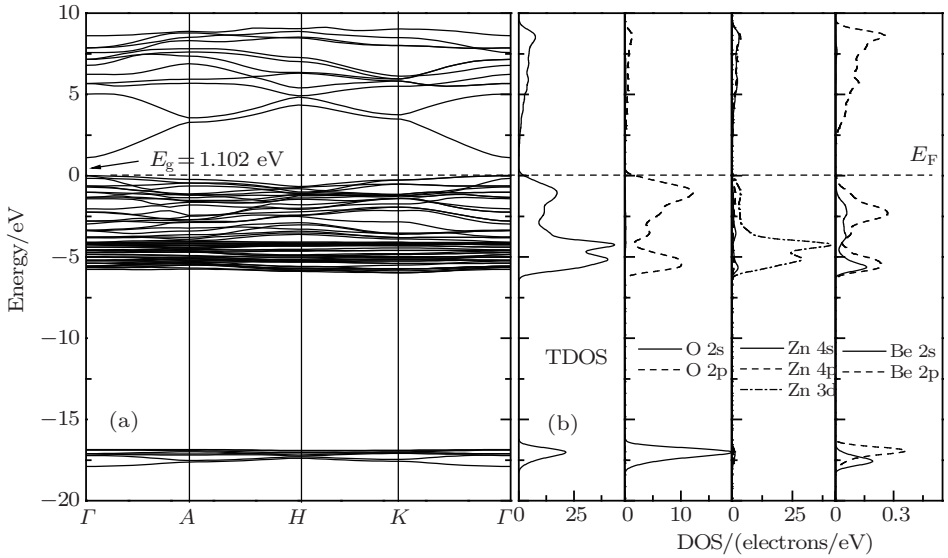


Fig. 3. Calculated band structure (a) and total DOS and partial DOS (b) of $Be_{0.125}Zn_{0.875}O$ alloy.

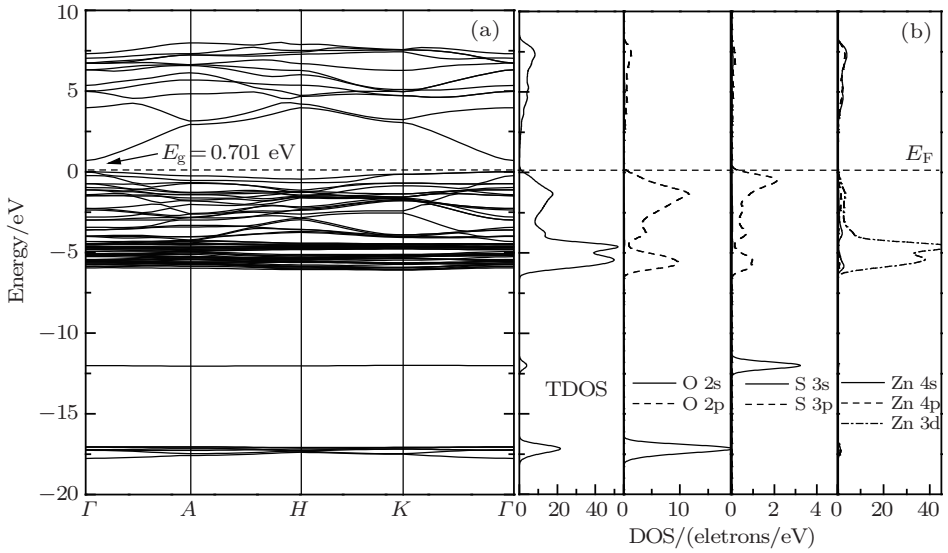


Fig. 4. Calculated band structure (a) and total DOS and partial DOS (b) of $ZnO_{0.875}S_{0.125}$ alloy.

The calculated band structure and density of state of $Be_{0.125}Zn_{0.875}O_{0.875}S_{0.125}$ quaternary alloy are shown in Fig. 5, it is clear that the $Be_{0.125}Zn_{0.875}O_{0.875}S_{0.125}$ alloy is also a direct bandgap material. The calculated band gap is 0.951 eV, which is smaller than that of $Be_{0.125}Zn_{0.875}O$ and larger than that of $ZnO_{0.875}S_{0.125}$. As shown in Fig. 5(b), the valence band of $Be_{0.125}Zn_{0.875}O_{0.875}S_{0.125}$ alloy consists of the lower valence band (from -18.5 eV to -16 eV), the

middle valence band (around −12 eV), and the upper valence band (from −6.6 eV to 0 eV), which is similar to the case of $ZnO_{0.875}S_{0.125}$. The upper valence band is composed mostly of the O 2p state, S 3p state, Zn 3d state, and a small number of Be 2s2p states, and the hybridization and the p–d repulsion make their electrons distribute mostly at the bottom of the upper valence band, but the S 3p state dominates the top of the valence band. The conduction band of the $Be_{0.125}Zn_{0.875}O_{0.875}S_{0.125}$ alloy is composed mainly of O 2p, S 3p, Zn 4s4p, and Be 2s2p states, but the electron distribution is diffusing and the Zn 4s state dominates the CBM. So the band gap of the $Be_{0.125}Zn_{0.875}O_{0.875}S_{0.125}$ alloy is determined by Zn 4s and S 3p states. It is interesting that the calculated lattice constant of the $Be_{0.125}Zn_{0.875}O_{0.875}S_{0.125}$ alloy is 3.315 Å for a and 5.292 Å for c, which are very close to those of ZnO compared with those of $Be_{0.125}Zn_{0.875}O$ and $ZnO_{0.875}S_{0.125}$ alloys. So it is possible to make the lattice constant of the $Be_xZn_{1-x}O_{1-y}S_y$ alloy matched with that of ZnO by choosing the appropriate doped content values x and y. It is important to develop a high-quality ZnO/$Be_xZn_{1-x}O_{1-y}S_y$ heterostructure for the ZnO-based device. $Be_{0.375}Zn_{0.625}O_{0.75}S_{0.25}$ quaternary alloy is the case that its lattice constant a is 3.274 Å, the lattice mismatch is only 0.24% compared with that of ZnO (see Table 1). In principle, if the lattice mismatch between two materials is less than 0.5%, the two materials are regarded as being perfectly matched.[29] So $Be_{0.375}Zn_{0.625}O_{0.75}S_{0.25}$ film may be grown easily on the ZnO (0001) substrate with a low defect density. The calculated band structure of $Be_{0.375}Zn_{0.625}O_{0.75}S_{0.25}$ quaternary alloy is shown in Fig. 6, obviously indicating that the alloy is also a direct bandgap material with a band gap of 1.096 eV, which is larger than that of ZnO.

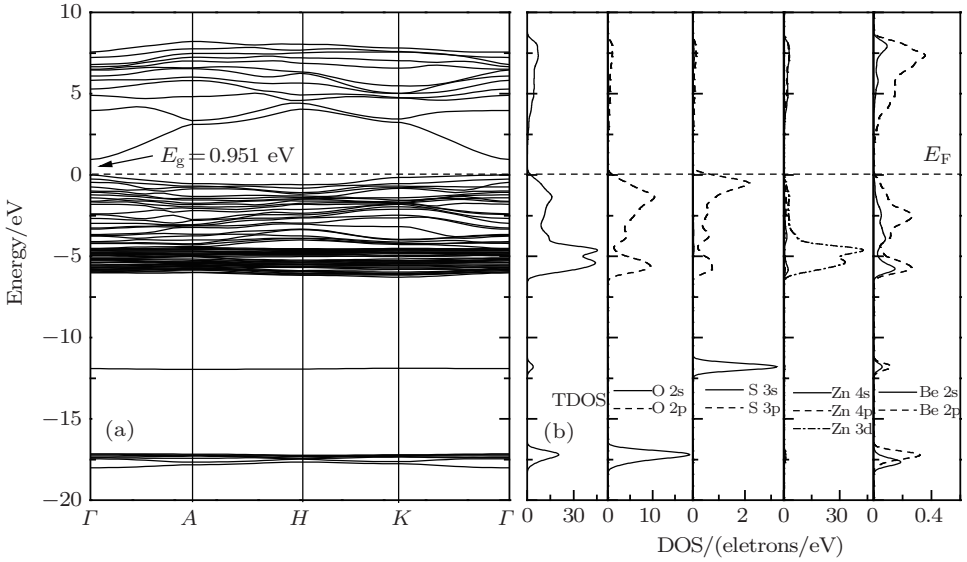


Fig. 5. Calculated band structure (a) and total DOS and partial DOS (b) of $Be_{0.125}Zn_{0.875}O_{0.875}S_{0.125}$ quaternary alloy.

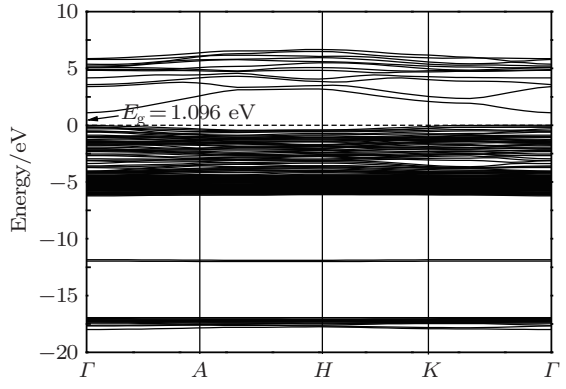


Fig. 6. Calculated band structure of $Be_{0.375}Zn_{0.625}O_{0.75}S_{0.25}$ quaternary alloy.

In order to evaluate the stability of the above-mentioned $Be_xZn_{1-x}O_{1-y}S_y$ alloy, the formation energies of the $Be_xZn_{1-x}O_{1-y}S_y$ alloys are calculated from the following formula:[13]

$$E_f(x,y) = E_{tot}(Be_xZn_{1-x}O_{1-y}S_y) - (1-x-y)E_{tot}(ZnO) - xE_{tot}(BeO) - yE_{tot}(ZnS), \quad (1)$$

where E_{tot} is the total energy of the $Be_xZn_{1-x}O_{1-y}S_y$ alloy with Be content x and S content y; E_{tot}(ZnO), E_{tot}(BeO), and E_{tot}(ZnS) are the total energies of ZnO, BeO, and ZnS in wurtzite structure, respectively. If $E_f(x,y)$ is negative, the $Be_xZn_{1-x}O_{1-y}S_y$ alloy is more stable than the binary alloys; if $E_f(x,y)$ is positive, the $Be_xZn_{1-x}O_{1-y}S_y$ alloy is less stable than the binary alloys. From Eq. (1), the formation energies of $Be_{0.125}Zn_{0.875}O$, $ZnO_{0.875}S_{0.125}$,

$Be_{0.125}Zn_{0.875}O_{0.875}S_{0.125}$, and $Be_{0.375}Zn_{0.625}O_{0.75}S_{0.25}$ alloys are 0.063 eV/pair, 0.084 eV/pair, 0.143 eV/pair, and 0.198 eV/pair, respectively. So the stability of the $Be_xZn_{1-x}O_{1-y}S_y$ alloy will decrease when doping Be and S into wurtzite ZnO. Due to the formation energies being small, the $Be_xZn_{1-x}O_{1-y}S_y$ alloys can be fabricated by optimizing the experiment condition.

3.3. Valence band alignment

Band offset is an important parameter in the heterostructures. Here, we investigate the valence band alignment by adopting the approach proposed by Tang *et al.*,[30] the calculation method has been described in detail elsewhere.[24]

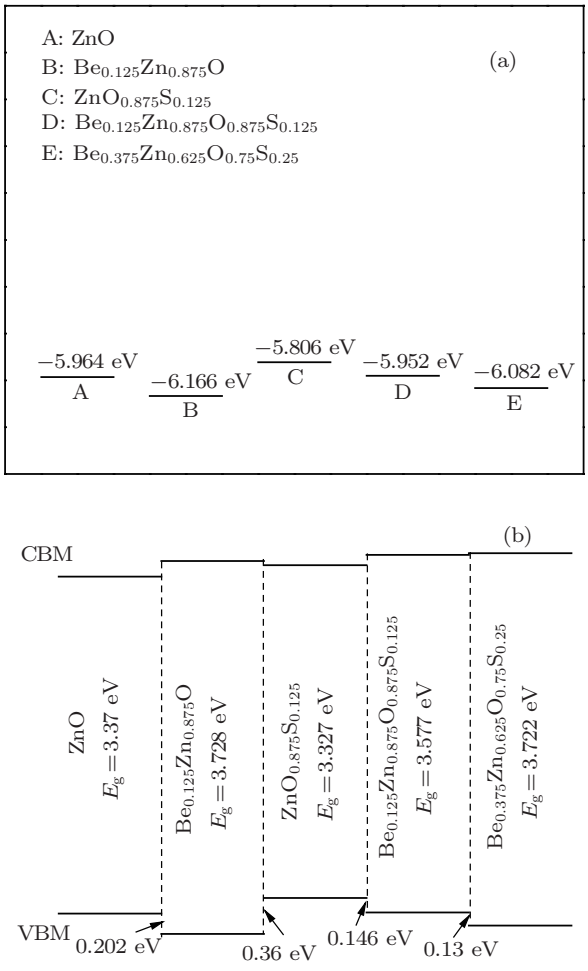


Fig. 7. Calculated relative energy of the VBM to the vacuum level (a) and band alignment (b) of $Be_xZn_{1-x}O_{1-y}S_y$ alloy. The band gaps are corrected by the scissors approximation.

Figure 7(a) shows that the relative energies of the VBM of $Be_xZn_{1-x}O_{1-y}S_y$ alloys to the vacuum level. It is evident that the calculated relative vacuum level to the VBM of ZnO is −5.964 eV, which is consistent with previous results.[24] Although the band gap of $Be_xZn_{1-x}O_{1-y}S_y$ is underestimated by DFT in the GGA and LDA, it can be corrected by the scissors approximation. The scissor value is set to be 2.626 eV according to the difference between the experimental value (3.37 eV[22]) and the calculated result (0.744 eV). The band alignment of $Be_xZn_{1-x}O_{1-y}S_y$ is plotted in Fig. 7(b) and the relative vacuum level of the VBM of ZnO serves as the reference. From Fig. 7(b) it follows that the VBM position of ZnO is higher than that of $Be_{0.125}Zn_{0.875}O$ and lower than that of $ZnO_{0.875}S_{0.125}$, which is in accordance with the above DOS analysis. The band gap of $Be_{0.375}Zn_{0.625}O_{0.75}S_{0.25}$ is 3.722 eV, larger than that of ZnO. It is noted that the VBM of $Be_{0.375}Zn_{0.625}O_{0.75}S_{0.25}$ is low and the CBM is high compared with those of ZnO alloy. So the $Be_{0.375}Zn_{0.625}O_{0.75}S_{0.25}$ alloy is suitable for serving as the blocking material to fabricate a high-quality ZnO/$Be_{0.375}Zn_{0.625}O_{0.75}S_{0.25}$ heterogeneous quantum well structure for a ZnO-based device.

4. Conclusion

The energy band properties, DOS, formation energy, and band alignment of the $Be_xZn_{1-x}O_{1-y}S_y$ alloy are investigated by the first-principles method. The results can be summarized as follows.

(i) The $Be_xZn_{1-x}O_{1-y}S_y$ alloy is a direct bandgap semiconductor, and its band gap is occupied by the Zn 4s state of the conduction band minimum (CBM) and the S 3p state of the valence band maximum (VBM). The band gap of $Be_xZn_{1-x}O_{1-y}S_y$ can be modulated by changing the doped content values x and y.

(ii) The lattice constant of the $Be_xZn_{1-x}O_{1-y}S_y$ alloy can be also adjusted by changing the doped content values x and y. When increasing the Be content x, the lattice constant of the $Be_xZn_{1-x}O_{1-y}S_y$ alloy becomes smaller, which is just contrary to the scenario when increasing the S content y in the $Be_xZn_{1-x}O_{1-y}S_y$ alloy.

(iii) According to the total energy and formation energy of the $Be_xZn_{1-x}O_{1-y}S_y$ alloy, its stability will declined when doping Be and S into wurtzite ZnO.

(iv) The lattice constant of the $Be_{0.375}Zn_{0.625}O_{0.75}S_{0.25}$ alloy is well matched with that of ZnO, and its band gap is 3.722 eV, larger than that of ZnO, so the $Be_{0.375}Zn_{0.625}O_{0.75}S_{0.25}$ alloy is suitable for serving as the blocking material for a high-quality ZnO-based device.

References

[1] Kligshirn C 1975 *Phys. Status Solidi B* **71** 547
[2] Park Y S, Litton C W, Collins T C and Reynolds D C 1966 *Phys. Rev.* **143** 512
[3] Thoms D G 1960 *J. Phys. Chem. Sol.* **15** 86
[4] Ryu Y R, Lee T S and White H W 2003 *Appl. Phys. Lett.* **83** 87
[5] Sanati M, Hart G L W and Zunger A 2003 *Phys. Rev. B* **68** 155210
[6] Fan X F, Sun H D, Shen Z X, Kuo J L and Lu Y M 2008 *J. Phys.: Condens. Matter* **20** 235221
[7] Makion T, Segawa Y, Ksaesdski M, Ohtomo A, Shiroki R, Tamura K, Yasuda T and Koinuma H 2001 *Appl. Phys. Lett.* **78** 1237
[8] Ryu Y R, Lee T S, Lubguban J A, Corman A B, White H W, Leem H J, Han M S, Park Y S, Youn C J and Kim W J 2006 *Appl. Phys. Lett.* **88** 052103

[9] Gan C K, Fan X F and Kuo J L 2010 *Comput. Mater. Sci.* **49** S29
[10] Su X Y, Si P P, Hou Q Y, Kong X L and Cheng W 2009 *Physica B: Condens. Matter* **404** 1794
[11] Shi H L and Duan Y 2008 *Eur. Phys. J. B* **66** 439
[12] Yang C, Li X M, Gu W D, Yu W D, Gao X D and Zhang Y W 2008 *Appl. Phys. Lett.* **93** 112114
[13] Zheng S W, Fan G H, Zhang Y, He M, Li S T and Zhang T 2012 *Acta Phys. Sin.* **61** 227101 (in Chinese)
[14] Ramasubramanian S, Thangavel R, Rajagopalan M and Kumar J 2009 *J. Alloys Compd.* **479** 414
[15] Shannon R D 1976 *Acta Cryst. A* **32** 751
[16] Fan X F, Shen Z X, Lu Y M and Kuo J L 2009 *New J. Phys.* **11** 093008
[17] Meyer B K, Polity A, Farangis B, He Y, Hasselkamp D, Krämer T and Wang C 2004 *Appl. Phys. Lett.* **85** 4929
[18] Segall M D, Lindan P, Probet M J, Pickard C J, Hasnip P J, Clark S J and Payne M C 2002 *J. Phys.: Condens. Matter* **14** 2717
[19] Perdew J, Burke K and Ernzerhof M 1996 *Phys. Rev. Lett.* **77** 3865
[20] Monkhorst H J and Pack J D 1976 *Phys. Rev. B* **13** 5188
[21] Fischer T H and Almlof J 1992 *J. Phys. Chem.* **96** 9768
[22] Yang Z H, Zheng J H, Zhai H J, Yang L L, Liu L and Gao M 2009 *Cryst. Res. Technol.* **44** 619
[23] Schleife A, Fuchs F, Furthmuller J and Bechstedt F 2006 *Phys. Rev. B* **73** 245212
[24] Tang X, Lü H F, Ma C Y, Zhao J J and Zhang Q Y 2008 *Acta Phys. Sin.* **57** 1066 (in Chinese)
[25] Shi L B, Li R B Cheng S and Li M B 2009 *Acta Phys. Sin.* **58** 6446 (in Chinese)
[26] Yoo Y Z, Jin Z W, Chikyow T, Fukumura T, Kawasaki M and Koinuma H 2002 *Appl. Phys. Lett.* **81** 3798
[27] Godby R W, Schluter M and Sham L J 1986 *Phys. Rev. Lett.* **56** 2415
[28] Fan X F, Zhu Z, Ong Y S, Lu Y M, Shen Z X and Kuo J L 2007 *Appl. Phys. Lett.* **91** 121121
[29] Xia J B, Zhu B F and Huang K 1995 *Semiconductor Superlattice Physics* (Shanghai: Shanghai Science and Technology Press) p. 19
[30] Tang X, Lu H F, Zhao J J and Zhang Q Y 2010 *J. Phys. Chem. Solids* **71** 336